Supporting Information

Mass Production of Lumenogenic Human Embryoid Bodies and Functional Cardiospheres using In-Air Generated Thin-shelled Microcapsules

Bas van Loo[1], Simone A. ten Den[2], Nuno Araújo-Gomes[1], Vincent de Jong[1], Rebecca R. Snabel[3], Maik Schot[1], José M. Rivera-Arbeláez[2,4], Gert Jan C. Veenstra[3], Robert Passier[2,5], Tom Kamperman[1,6], and Jeroen Leijten[1]

[1] University of Twente, TechMed Centre, Department of Developmental BioEngineering, Enschede, The Netherlands

[2] University of Twente, TechMed Centre, Department of Applied Stem Cell Technology, Enschede, The Netherlands

[3] Radboud University, Radboud Institute for Molecular Life Sciences, Faculty of Science, Department of Molecular Developmental Biology, Nijmegen, The Netherlands

[4] University of Twente, TechMed Centre, Max Planck Center for Complex Fluid Dynamics, BIOS Lab-on-a-Chip Group , Enschede, The Netherlands

[5] Leiden University Medical Centre, Department of Anatomy and Embryology, Leiden, Netherlands

[6] IamFluidics B.V., De Veldmaat 17, 7522NM Enschede, The Netherlands.

Supplemental figures

Supplemental figures

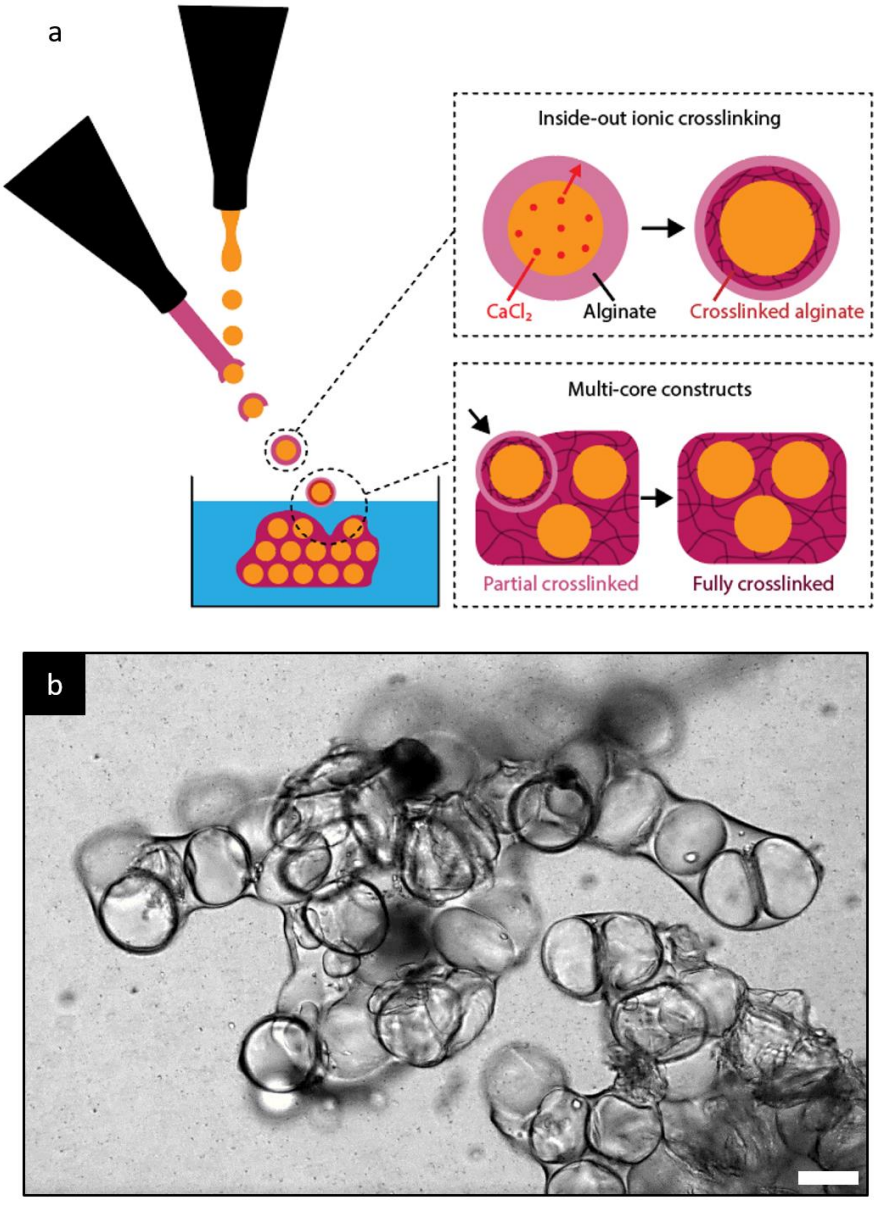

Figure S1. In Air microfluidics using a two-nozzle setup results in formation of uncontrolled multi-compartment microparticles. (a) Schematic of two-nozzle setup, inside-out crosslinking process, and mechanism by which multi-compartment microparticles are formed. (b) Microphotograph of formed microparticle using two-nozzle in-air microfluidics. Scale bar represents 200 µm.

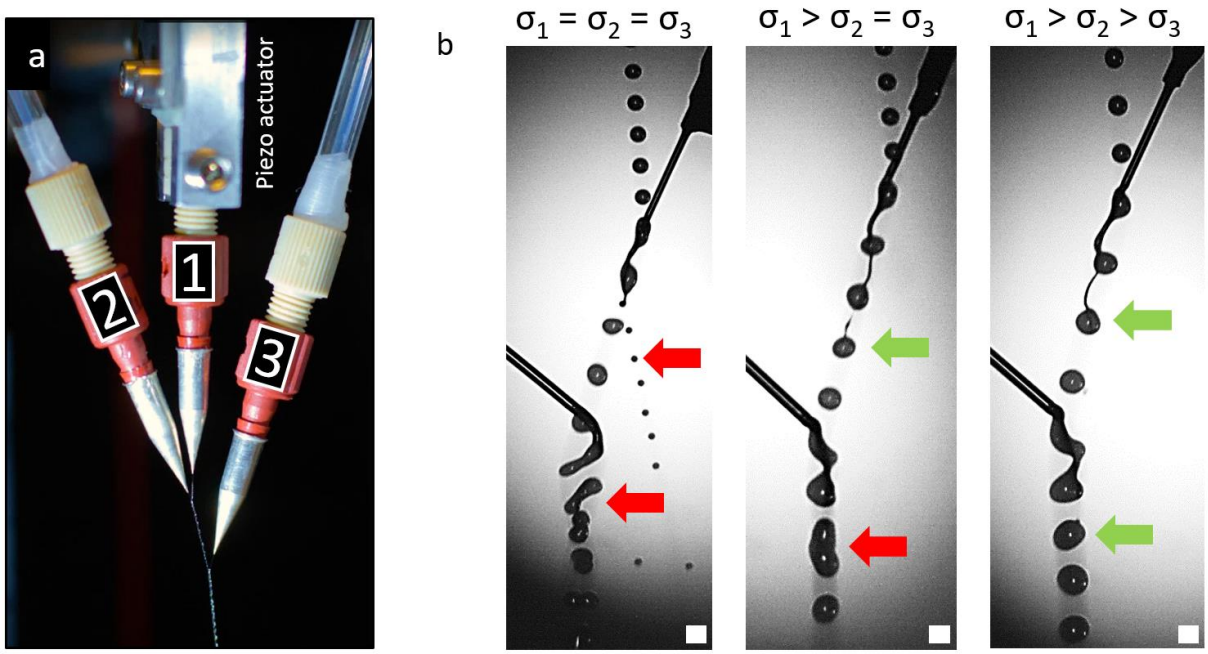

Figure S2. In Air microfluidics three-nozzle setup for In Air droplet encapsulation. (a) Photograph of a three nozzle In Air microfluidics setup, with a piezo-electric actuator attached to the first nozzle. (b) Microphotographs of the encapsulation process with $\sigma_1 = \sigma_2 = \sigma_3$, $\sigma_1 > \sigma_2 = \sigma_3$ and $\sigma_1 > \sigma_2 > \sigma_3$. Red arrows indicate spraying and improper encapsulation, green arrows indicate proper encapsulation. Scale bar represents 200 µm.

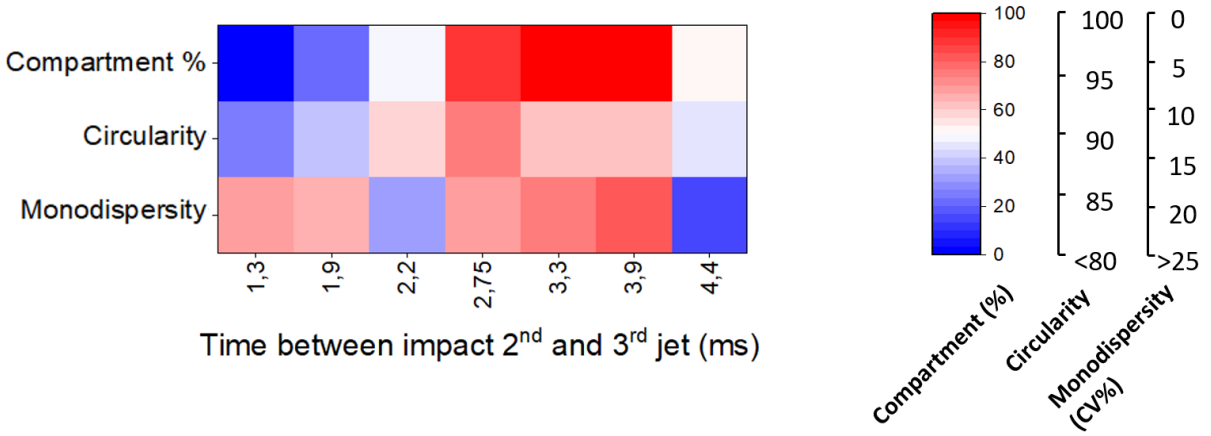

Figure S3. Third jet coalescence location dictates hollow microcapsule formation. Effect of in-air flight time before third jet coalescences with the droplet train as analyzed in terms of percentage of single compartment, circularity, and monodispersity of produced microparticles (n>85).

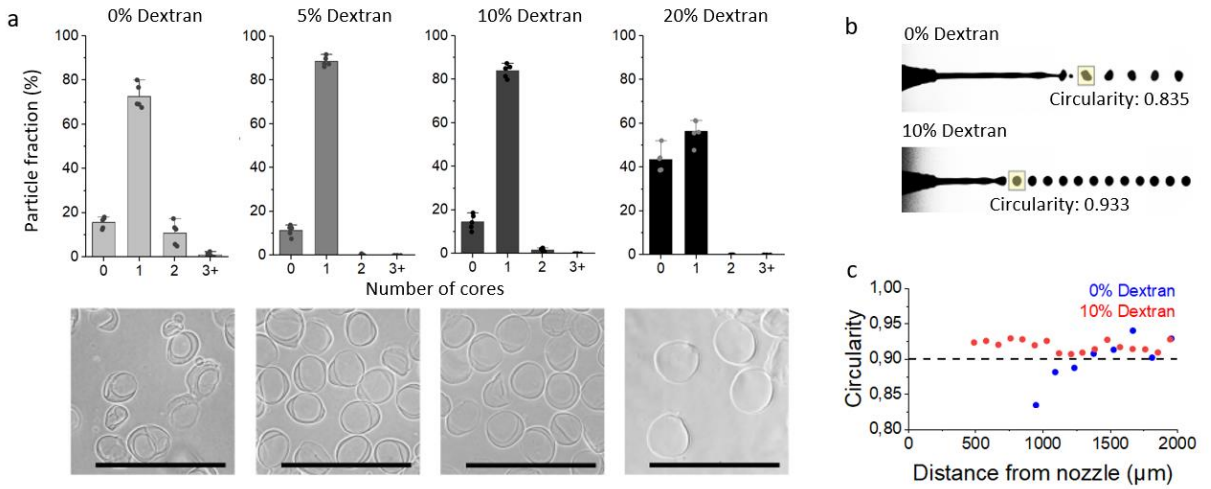

Figure S4. Effect of dextran in core liquid on hollow microcapsule formation. (a) Number of hollow compartments per microparticle using dextran core liquid concentrations of 0%, 5%, 10%, and 20%, including corresponding microphotographs (n=60). Data is presented as mean values +/- SD. (b) Microphotographs and (c) quantification of circularity of formed droplets with and without 10% dextran. Scale bar represents 400 µm.

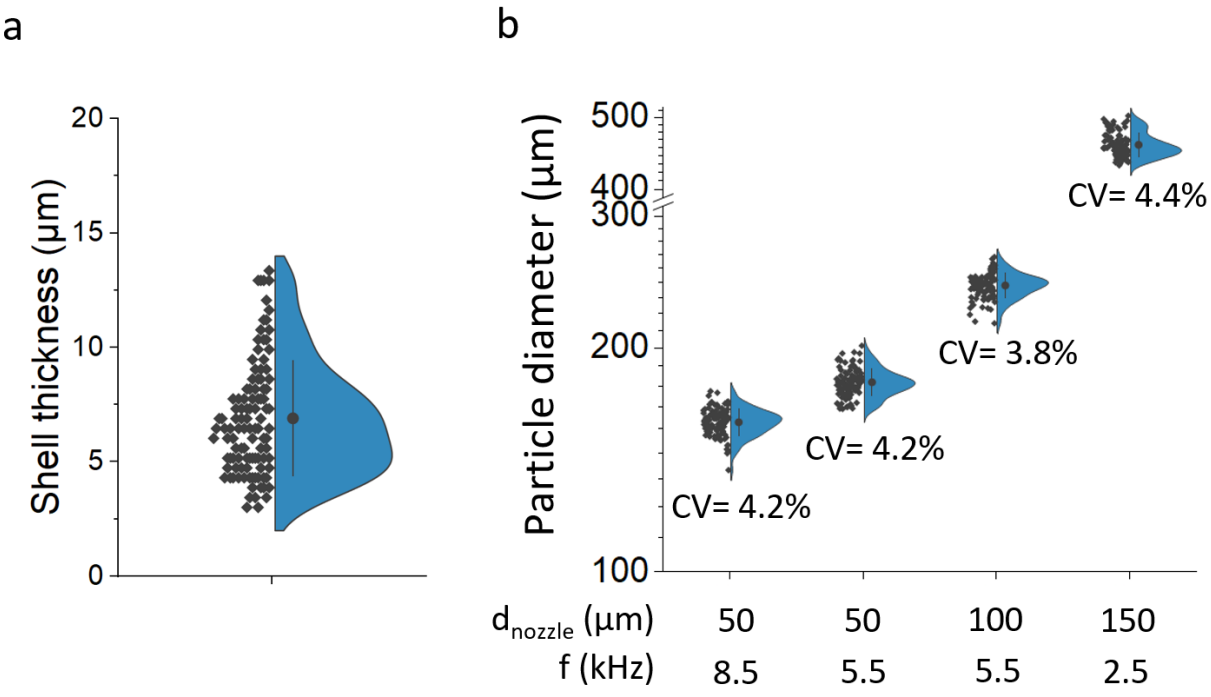

Figure S5. Hollow microcapsule morphology. (a) Quantification of shell thickness of in-air produced microcapsules (n=107). Data is presented as mean values +/- SD. (b) Quantification of microcapsule diameter and monodispersity using different nozzle sizes and different piezo-electric actuator frequencies (n=100). Data is presented as mean values +/- SD.

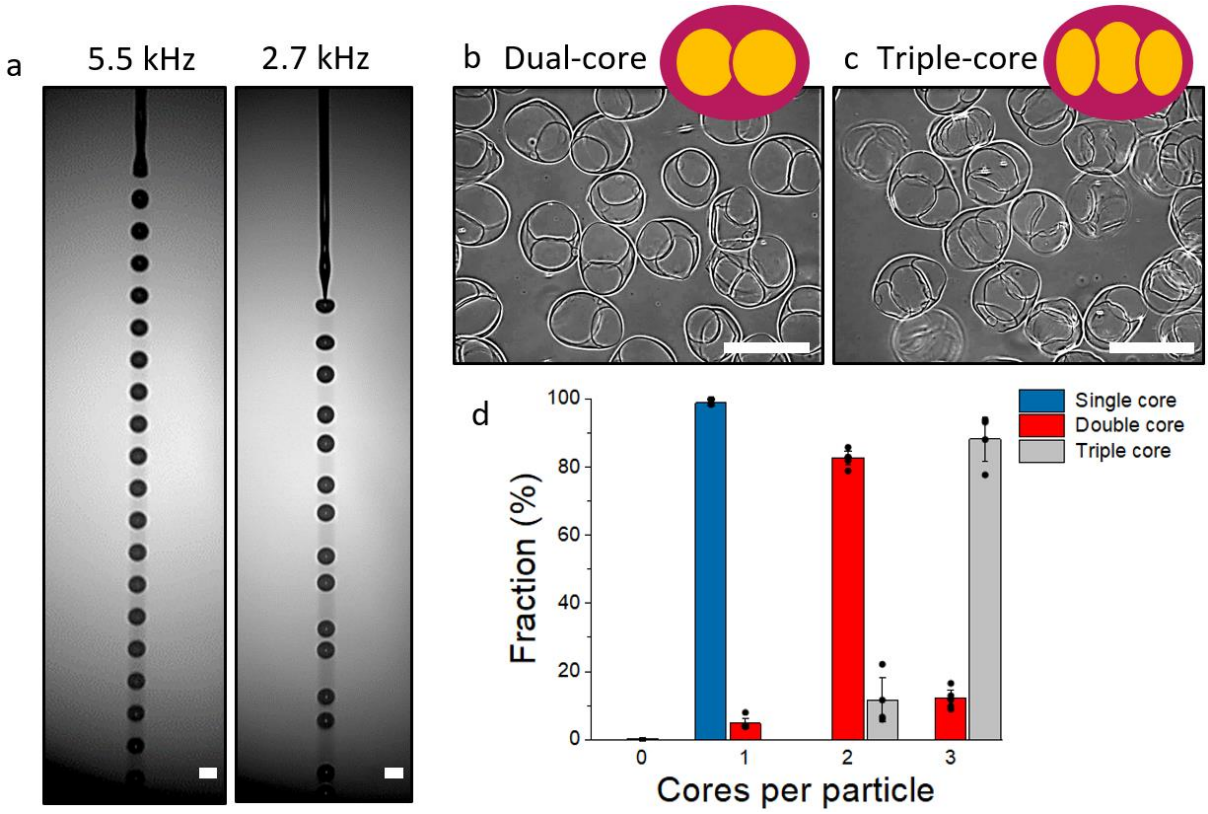

Figure S6. Controlled production of multi-core microparticles by adjusting piezo-actuator frequency. (a) Microphotographs of droplet formation at 5.5 kHz and 2.7 kHz. (b) Microphotograph of dual-core microcapsules (c) and triple-core microcapsules. (d) Quantification of percentage single-, dual-, and triple-core microcapsules (n=169 microparticles). Data is presented as mean values +/- SD. Scale bar represents 200 µm.

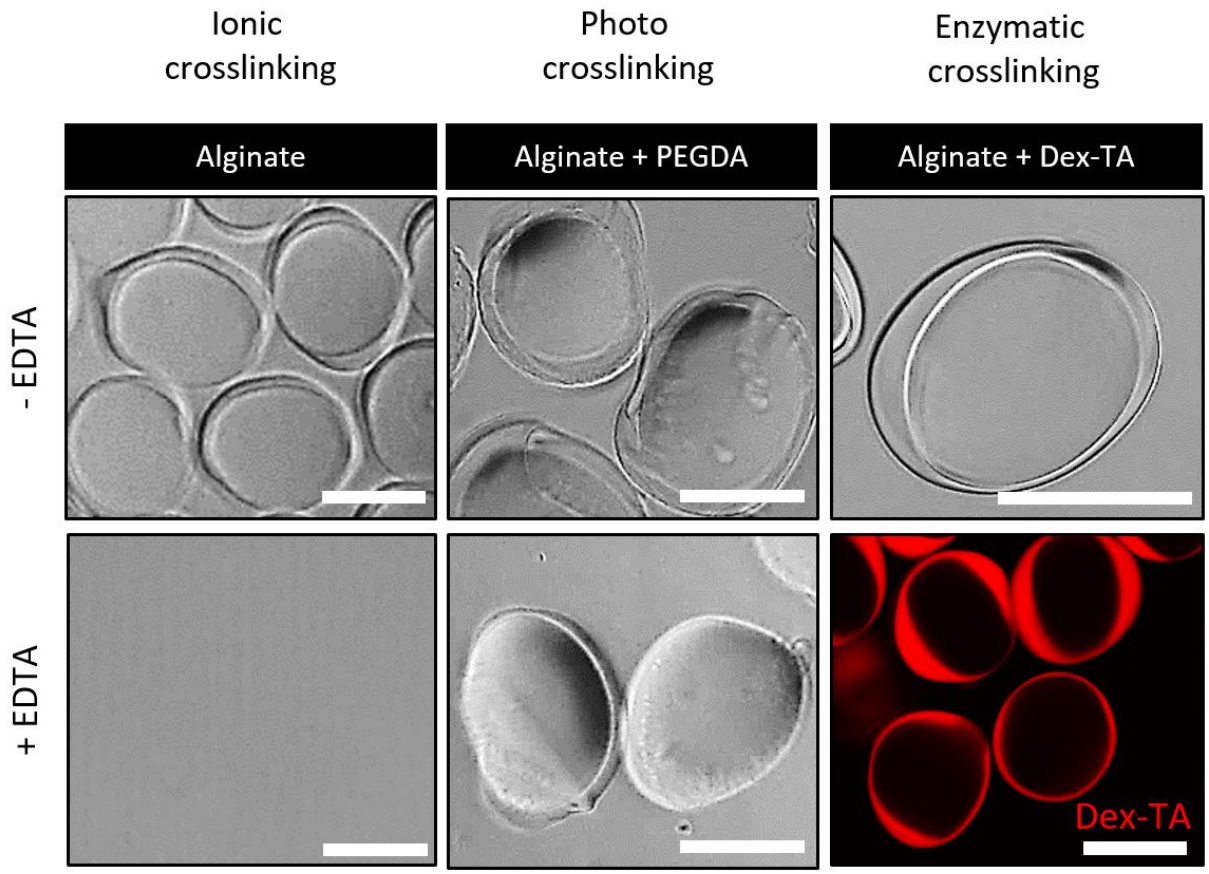

Figure S7. In Air production of microcapsules using photocrosslinkable and enzymatic crosslinkable materials. Microphotographs of ionically crosslinked alginate microcapsules, photocrosslinked PEGDA microcapsules, and enzymatic crosslinked dextran-tyramine microcapsules, before and after EDTA treatment. Dex-TA microcapsules post-EDTA were stained with ethidium homodimer (red). Scale bar represent 100 µm.

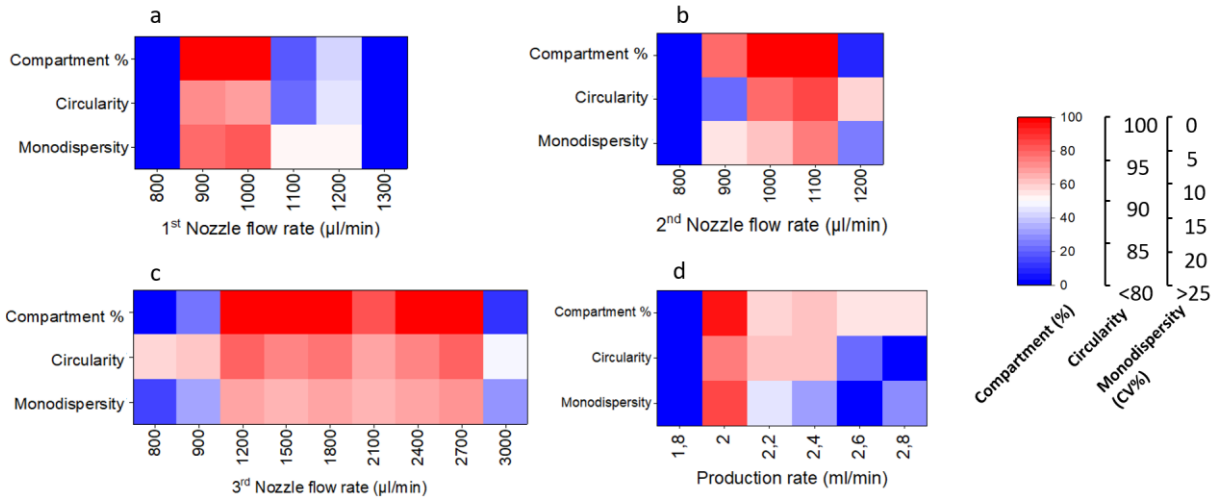

Figure S8. Flow rate optimization for microcapsules production. Quantification of the percentage of microparticles containing a single compartment, circularity of formed microparticles, and microparticle monodispersity. Setup used: Nozzle 1 (50 µm) at 900 µl/min, nozzle 2 (50 µm) at 1100 µl/min, nozzle 3 (100 µm) at 1500 µl/min. (a) Effect of first nozzle flow rate on microparticle formation (n=100). (b) Effect of second nozzle flow rate on microparticle formation (n=100). (c) Effect of third nozzle flow rate on microparticle formation (n=100). (d) Effect of total production flow rate on microparticle formation (n=100). Ratios between flow rates were kept constant at the ratio described above.

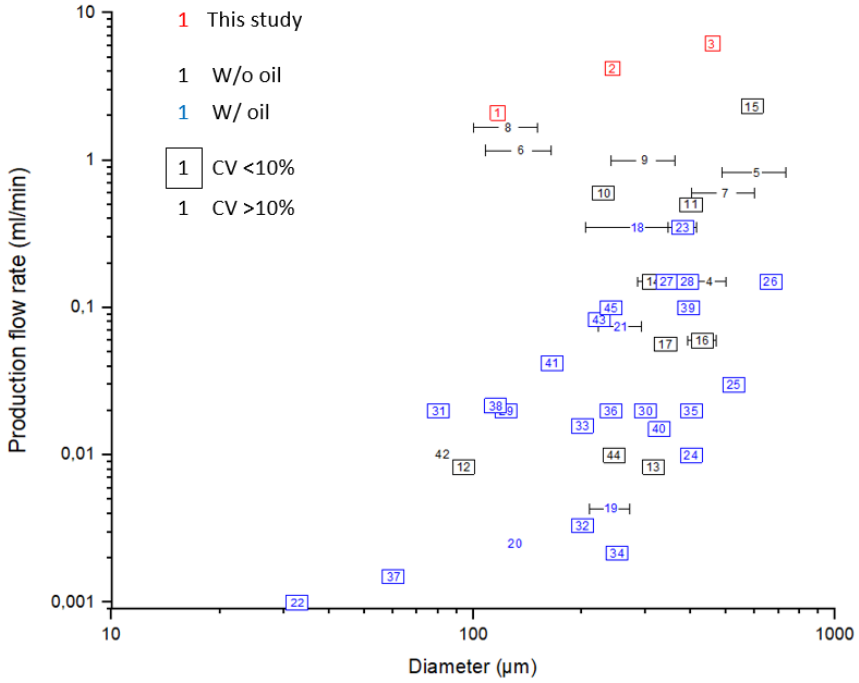

1-3	This work
4	Aghdam et al.[86]
5	Correia et al.[44]
6	Alessandri et al.[46]
7	Ma et al.[47]
8	Alessandri et al.[45]
9	Rutkowski et al.[48]
10	Sakai et al.[48]
11	Ren et al.[69]
12-13	Song et al.[69]
14	Zhao et al.[79]
15	Domejean et al.[65]
16	Rao et al.[40]
17-18	Nguyen et al.[43]
19	Agarwal et al.[41]
20	Kim et al.[67]
21	Ashida et al.[64]
22	Seuss et al.[64]
23	Agarwal et al.[63]
24	Siltanen et al.[71]
25	Zhao et al.[78]
26-28	Watanabe et al.[75]
29-31	van Loo et al.[74]
32	Sun et al.[73]
33	Hu et al.[66]
34	Xie et al.[76]
35	Yang et al.[77]
36	Kamperman et al.[54]
37	Yu et al.[80]
38	Lin et al.[68]
39	Fattahi et al.[85]
40	Zhu et al.[84]
41	Jeong et al.[83]
42	Mytnyk et al.[49]
43	Wang et al.[81]
44	Liu et al.[39]
45	Liu et al.[82]

Figure S9. Literature study for continuously produced hollow core-shell microcapsules.

Elaboration of figure 2l with corresponding studies per datapoint.

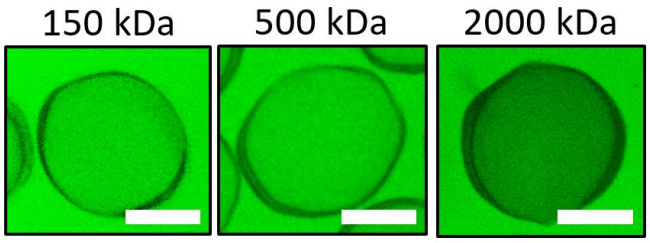

Figure S10. Permeability of microcapsules.

Fluorescent confocal micrographs of microcapsules incubated for 30 minutes in Dextran-FITC containing solutions of 150 kDa, 500 kDa and 2000 kDa. Representative micrographs out n=3 experiments. Scale bars represent 100 µm.

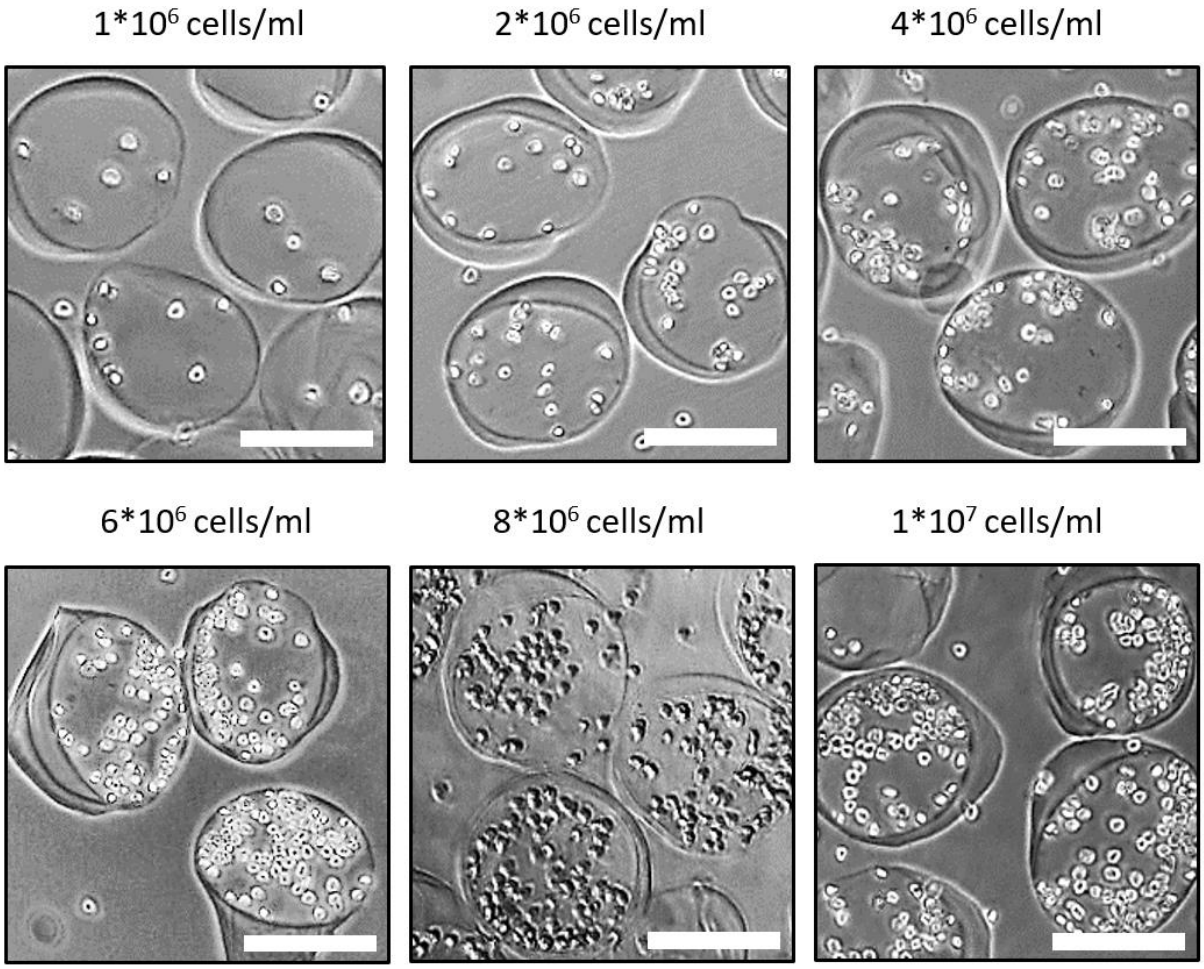

Figure S11. In Air microencapsulation of 3T3 Fibroblast within alginate microcapsules. Microphotographs of 3T3 fibroblast-laden microcapsules produced using a variety of cell concentrations. Representative micrographs out n=3 experiments. Scale bars represent 200 µm.

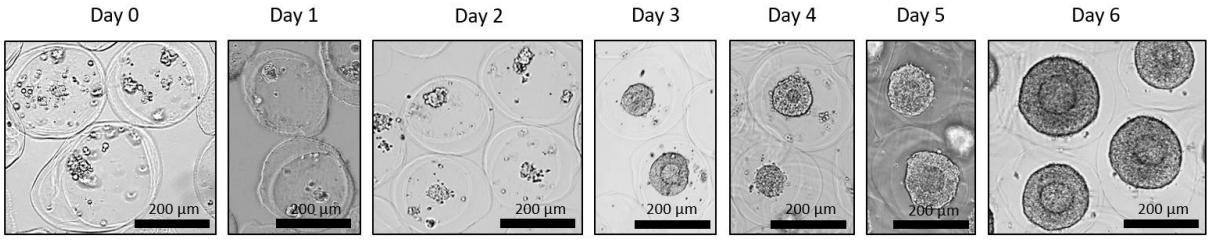

Figure S12 Embryoid body formation by in-air microcapsulated hPSCs. Microphotographs of encapsulated hPSCs show aggregation and lumenogenesis. Representative micrographs out n=3 experiments. Scale bar represents 200 µm.

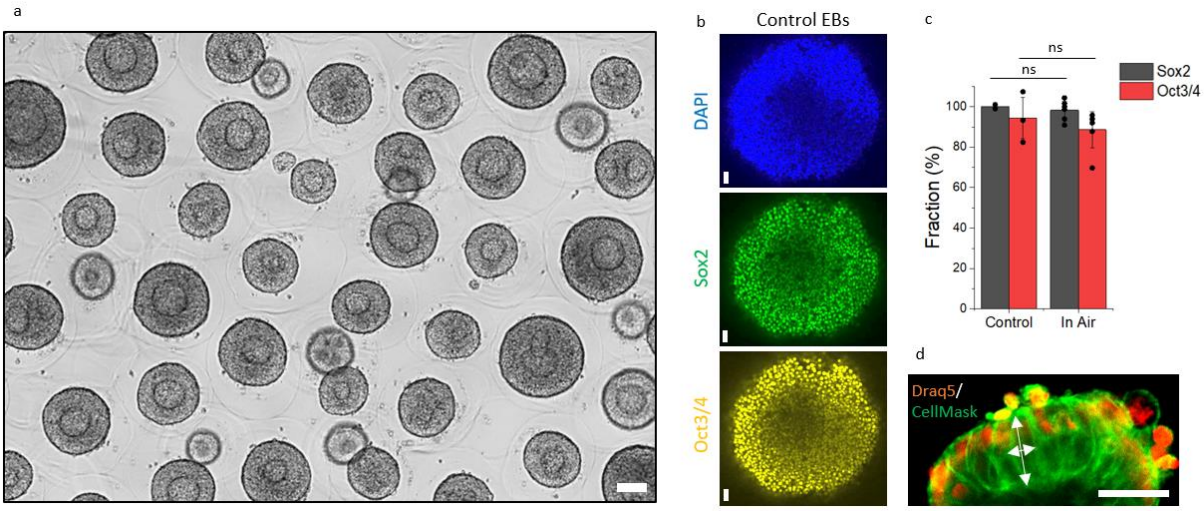

Figure S13. Mass production of embryoid body by in-air microcapsulating hPSCs. (a) Microphotograph of EBs formed within in-air produced alginate microcapsules. Representative micrographs out n=3 experiments. (b) Fluorescence microphotograph of EBs produced using microwells with 5000 cells/microwell, which were stained with DAPI for nuclei (blue), SOX2 (green), and OCT3/4 (yellow) for pluripotency. (c) Quantification and comparison of pluripotency by percentage of cells positive for SOX2 and OCT3/4 between EBs produced with conventional microwells or In Air microfluidics (n=300 cells). Data is presented as mean values +/- SD. Significance was determined based on one-way Anova analysis. Significance was determined based on one-way Anova analysis.

Significance of p <0.05 is indicated by *. (d) Confocal microphotograph of an EB with its nucleus stained with Draq5 (orange) and its cell membrane stained with CellMask (green). Scale bars represent 50 µm.

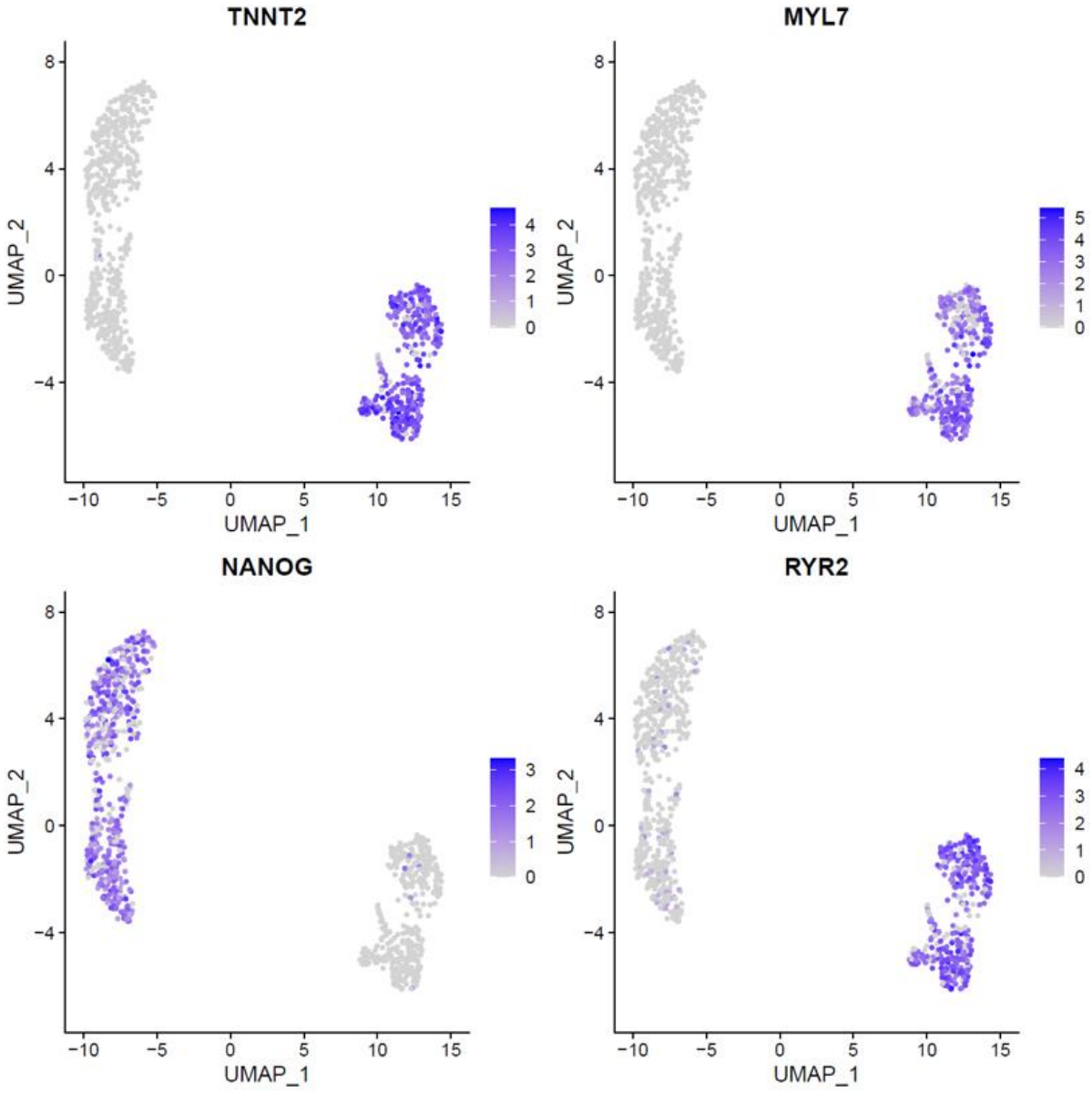

Figure S14. Single cell RNA sequencing UMAP plots for pluripotency and cardiac markers. Heatmap of NANOG, TNNT2, MYL7 and RYR2 gene expression in UMAP plots.

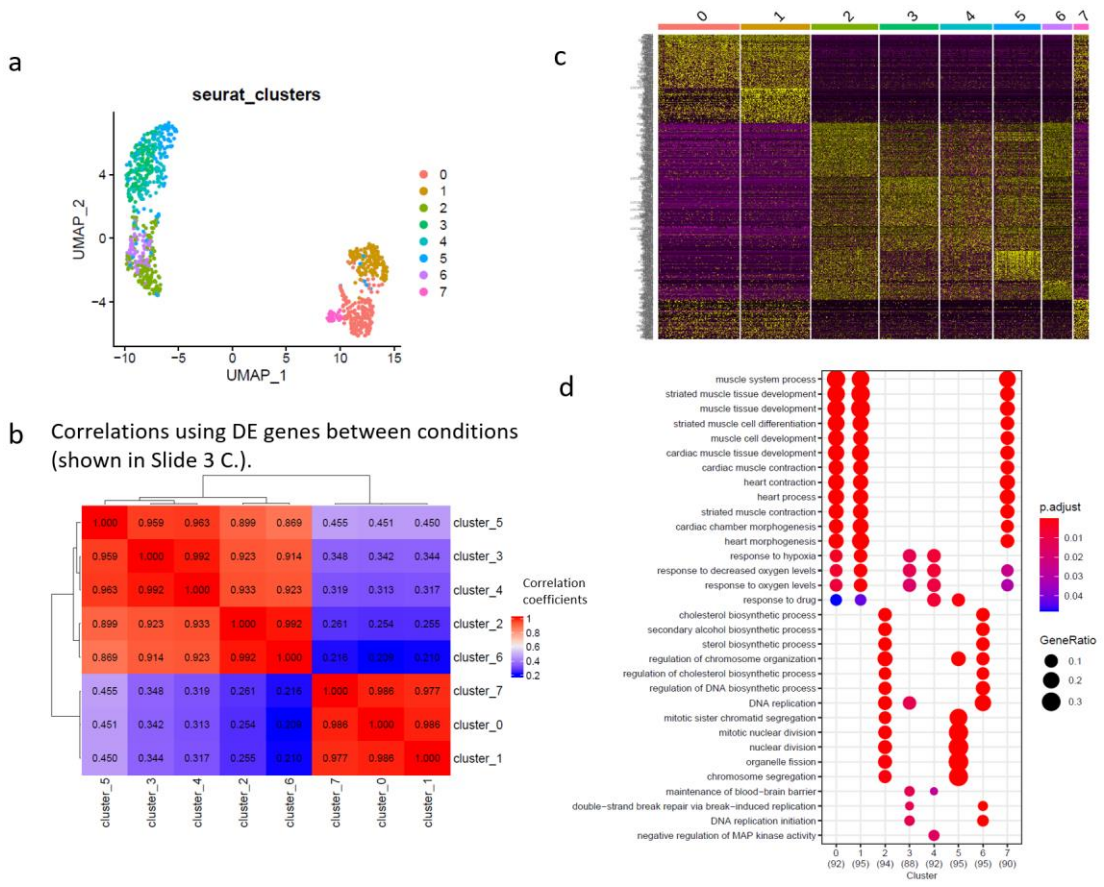

115

116 **Figure S15. Single cell RNA sequencing Seurat cluster data.** (a) Seurat clusters. (b) Correlation using
117 differential expression genes between conditions. (c) Heatmap of marker genes corresponding to
118 identified clusters. (d) Gene ontology heatmap of differential genes per cluster. P-adjust corrected
119 using Benjamini-Hochberg correction for multiple comparisons.

120

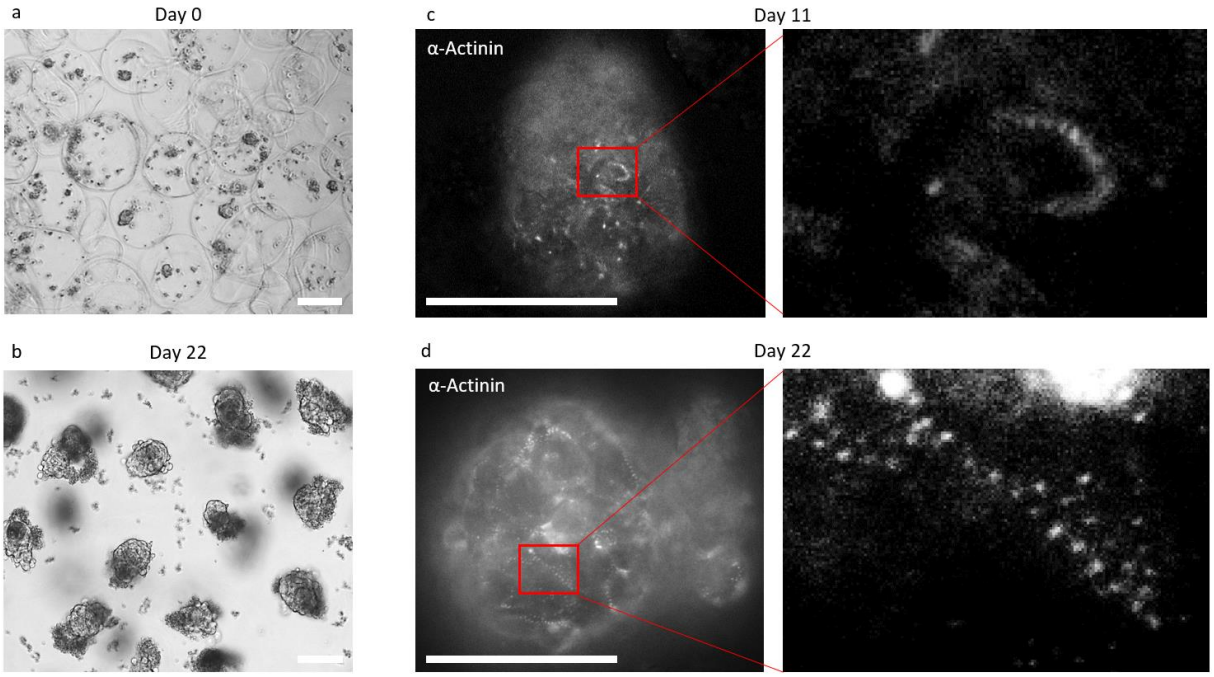

Figure S16. Functional *human* cardiospheres produced in mass using in-air microfluidics. (a) Microphotograph of encapsulated *human* pluripotent stem cells immediate after microencapsulation. (b) Microphotograph of encapsulated cardiospheres after 22 days of cardiac differentiation. Fluorescence microphotograph of α-actinin reporter in differentiated cardiomyocytes cultured after (c) 11 days and (d) 22 days of culture. Scale bars represent 100 µm.